


## ARTICLE

# The contribution of nearshore oceanography to temporal variation in larval dispersal

Katrina A. Catalano<sup>1</sup> | Elizabeth J. Drenkard<sup>2,3</sup> | Enrique N. Curchitser<sup>2</sup> |  
 Allison G. Dedrick<sup>1</sup> | Michelle R. Stuart<sup>1</sup> | Humberto R. Montes Jr.<sup>4</sup> |  
 Malin L. Pinsky<sup>1,5</sup> 

<sup>1</sup>Department of Ecology, Evolution, and Natural Resources, Rutgers University, New Brunswick, New Jersey, USA

<sup>2</sup>Department of Environmental Sciences, Rutgers University, New Brunswick, New Jersey, USA

<sup>3</sup>NOAA Geophysical Fluid Dynamics Laboratory, Princeton, New Jersey, USA

<sup>4</sup>Visayas State University, Baybay City, Leyte, Philippines

<sup>5</sup>Department of Ecology & Evolutionary Biology, University of California Santa Cruz, Santa Cruz, California, USA

## Correspondence

Malin L. Pinsky

Email: [mpinsky@ucsc.edu](mailto:mpinsky@ucsc.edu)

## Funding information

Alfred P. Sloan Foundation, Grant/Award Number: BR2014-044; Oak Ridge Associated Universities (Ralph E. Powe Junior Faculty Enhancement Award); National Science Foundation, Grant/Award Numbers: OCE-1426891, OCE-1430218, OISE-1743711; Rutgers University

**Handling Editor:** Mark A. Hixon

## Abstract

Patterns of population connectivity shape ecological and evolutionary phenomena from population persistence to local adaptation and can inform conservation strategy. Connectivity patterns emerge from the interaction of individual behavior with a complex and heterogeneous environment. Despite ample observation that dispersal patterns vary through time, the extent to which variation in the physical environment can explain emergent connectivity variation is not clear. Empirical studies of its contribution promise to illuminate a potential source of variability that shapes the dynamics of natural populations. We leveraged simultaneous direct dispersal observations and oceanographic transport simulations of the clownfish *Amphiprion clarkii* in the Camotes Sea, Philippines, to assess the contribution of oceanographic variability to emergent variation in connectivity. We found that time-varying oceanographic simulations on both annual and monsoonal timescales partly explained the observed dispersal patterns, suggesting that temporal variation in oceanographic transport shapes connectivity variation on these timescales. However, interannual variation in observed mean dispersal distance was nearly 10 times the expected variation from biophysical simulations, revealing that additional biotic and abiotic factors contribute to interannual connectivity variation. Simulated dispersal kernels also predicted a smaller scale of dispersal than the observations, supporting the hypothesis that undocumented abiotic factors and behaviors such as swimming and navigation enhance the probability of successful dispersal away from, as opposed to retention near, natal sites. Our findings highlight the potential for coincident observations and biophysical simulations to test dispersal hypotheses and the influence of temporal variability on metapopulation persistence, local adaptation, and other population processes.

## KEYWORDS

dispersal, dispersal kernel, interannual variability, larvae, marine ecology, metapopulation, oceanography, reef fish

This is an open access article under the terms of the [Creative Commons Attribution-NonCommercial](https://creativecommons.org/licenses/by-nc/4.0/) License, which permits use, distribution and reproduction in any medium, provided the original work is properly cited and is not used for commercial purposes.

© 2024 The Author(s). *Ecology* published by Wiley Periodicals LLC on behalf of The Ecological Society of America.

## INTRODUCTION

Dispersal is a foundational process that affects nearly all ecological and evolutionary phenomena, including population persistence, community composition, and spatial genetic structure (da Silva Carvalho et al., 2015; Hastings & Botsford, 2006; Resasco & Fletcher, 2021; Tigano & Friesen, 2016). Recent empirical work demonstrates that population connectivity can vary interannually and seasonally, but a general mechanistic understanding of connectivity variation and its consequences is lacking (Catalano et al., 2021; Harrison et al., 2020; Saenz-Agudelo et al., 2012). Most organisms with environmentally driven dispersal (e.g., by wind or water, including many arthropods, plants, and marine species) likely experience connectivity variation, but it can be difficult to disentangle the relative contributions of the abiotic environment and demography (such as birth and survival rates) to the observed variation in dispersal, thus impeding the development of model frameworks (Shoemaker et al., 2020; Sullivan et al., 2021).

For organisms with physically driven dispersal, environmental variation affects the fluid circulation that structures the dispersal pathways for any given individual (Shoemaker et al., 2020; Watson et al., 2010). However, a dearth of dispersal observations accompanied by environmental data on corresponding spatial and temporal scales has hindered understanding the contribution of environmental variation to observed connectivity variation. A mechanistic understanding of dispersal variation may help to explain phenomena such as recruitment, community turnover, and genetic variation (Bani et al., 2019; Pringle et al., 2011; Sullivan et al., 2021). Elucidating the mechanisms of dispersal variation will also enhance predictive models to guide conservation and management (Shoemaker et al., 2020).

Empirical work has revealed complex and varied drivers of dispersal variation (Berumen et al., 2012; Catalano et al., 2021; Harrison et al., 2020; Hogan et al., 2012; Pusack et al., 2014; Saenz-Agudelo et al., 2012; Stillman et al., 2022). Within specific systems like coral reef clownfishes (genus *Amphiprion*), connectivity patterns can be mostly consistent across years in a sheltered bay and differ substantially across years for a population along an open coastline (Catalano et al., 2021; Saenz-Agudelo et al., 2012). While this contrast may be attributable to differing ocean conditions, connectivity variation in other systems highlights the role of biological factors. For example, interannual fluctuations in the biomass of the temperate kelp *Macrocystis pyrifera* are driven by strong interannual variation in kelp fecundity, rather than dispersal variation (Castorani et al., 2017). As more empirical studies of connectivity variation become available, disentangling the

relative contribution of demographic and environmental variation to emergent connectivity patterns will be crucial to understanding dynamic population connectivity.

Nearshore marine systems provide a unique opportunity to elucidate the mechanisms of dispersal variation. Many marine organisms disperse at the start of their lives as propagules entrained in the water column before settling in the habitat patch where they will spend the rest of their lives (White et al., 2019). While many propagules demonstrate remarkable behaviors that can affect their movement, dispersal takes place in the stochastic oceanographic environment where the interaction of moving water with the ocean floor and atmosphere creates spatial heterogeneity and chaotic dynamics at the sub- and mesoscales relevant to propagule dispersal (Leis et al., 2011; Mitarai et al., 2008; Siegel et al., 2008). A single dispersal event then represents one sample from a probability distribution of possible pathways at a given time and place (Gaines & Bertness, 1992; Mitarai et al., 2008; Siegel et al., 2008). For example, the oceanographic features that cause spatially heterogeneous transport often strengthen or weaken on a seasonal basis (Paris & Cowen, 2004; Schunter et al., 2011; White et al., 2010). Differences in thermohaline structure and convergence or divergence zones can create fronts that act as a dynamic boundary for particles on either side. When active, these fronts can decrease connectivity between populations that are otherwise a short distance from each other (Gilg & Hilbish, 2003; Wolanski et al., 1989). Turbulent mesoscale and submesoscale eddies may transport propagules offshore, while strong alongshore currents may facilitate dispersal between distant populations or interact with eddies and facilitate propagule retention (Mitarai et al., 2008; Paris et al., 2007; Pringle et al., 2011). Simulations have demonstrated that stochastic oceanographic transport can, in theory, drive variation in connectivity on timescales ranging from days to years, but these expectations need to be validated empirically (Mitarai et al., 2008; Siegel et al., 2008).

Coupling oceanographic simulations of connectivity with empirical dispersal observations provides a powerful hypothesis-testing framework. Studies of marine dispersal often either simulate dispersal based on oceanographic circulation models or observe in situ connectivity, with tagging to determine the origin of sampled individuals (Cowen & Sponaugle, 2009). Both approaches have limitations. Genetic data can identify net dispersal trajectories by identifying parent-offspring relationships but are limited to the time of sampling and can only describe connectivity for individuals that survive dispersal and post-recruitment to the point of sampling (Bode et al., 2018; Burgess et al., 2014). Alternatively, biophysical simulations can use species-specific trait data to simulate

connectivity patterns with particles as proxies for dispersing individuals (Bode et al., 2019). These particle simulations can be run with fine-resolution oceanographic models that recreate circulation patterns for the location and time period of interest, in effect creating a hypothesis for dispersal (Mitarai et al., 2008; Siegel et al., 2008). Accurately recreating the mesoscale patterns and larval dispersal trajectories for a given year is difficult, particularly in data-limited regions of the world, and so average conditions across multiple years may be a more appropriate representation of dispersal conditions (Riginos & Liggins, 2013). Recent efforts to statistically integrate these approaches for the coral reef fish *Plectropomus maculatus* have demonstrated that tagging data can be used to validate biophysical simulations and evaluate potential biological mechanisms driving observed dispersal patterns (Bode et al., 2019; Burgess et al., 2022). This research has demonstrated that biophysical simulations have the power to simulate observed dispersal events. An important extension will be to identify whether oceanographic flow contributes to empirical connectivity variation.

To explore the contribution of variable oceanographic transport to temporal connectivity variation, we leveraged three years (2012–2014) of coincident biophysical simulations and direct observations of *Amphiprion clarkii* (yellowtail clownfish) dispersal in the eastern Camotes Sea along the coast of Leyte, Philippines. We hypothesized that temporal variation in oceanographic flow contributed to annual and seasonal variation in observed connectivity patterns and assessed dispersal patterns from simulations using average, annual, and seasonal oceanographic conditions against observed individual larval dispersal events. We also tested the ability of our high-resolution biophysical simulations to capture the observed magnitude and spatial scale of connectivity variation.

## MATERIALS AND METHODS

### Study system

The Philippine Archipelago sits in the Coral Triangle, an equatorial region at the confluence of the Pacific and Indian Ocean basins. The Philippines has a tropical climate with seasonal monsoons (Lau & Yang, 1997). The northeast monsoon (Amihan) occurs during November–May and is characterized by low rainfall and northeasterly winds. The southwest monsoon (Habagat) brings heavier rainfall during June–October, southwesterly winds, and cyclones.

The Camotes Sea is a small sea in the Central Visayas region within the archipelago and is about 80 km wide east–west and 90 km north–south (Figure 1). The sea is

sheltered from the major circulation of the North Equatorial Current by the island of Leyte to the east and from the South China and Sulu Seas to the west by the islands of Cebu and Negros (Castruccio et al., 2013). Cebu Strait to the southwest and the Canigao Channel to the southeast connect to the Bohol Sea. The Camotes Sea also connects to the Visayan Sea to the northwest.

### Genetic dispersal observations

The clownfish *A. clarkii* occupies sea anemones on coral reefs. The largest two adults in an anemone breed, laying eggs on benthic substrate nearby (Ochi, 1989). After about six days of development, eggs hatch into larvae that disperse with ocean currents for 8–10 days (Holtswarth et al., 2017). Juveniles that settle back to an anemone generally remain there for the rest of their lives, making clownfish ideal for dispersal studies because the distance between a parent and its offspring indicates an individual's net dispersal distance. *A. clarkii* spawn on a lunar cycle (full moon) all year long and produce the most eggs from November to May (Holtswarth et al., 2017). Generation time is around five years based on growth and maturity in this species (Dedrick et al., 2021; Moyer, 1986; Ochi, 1986). Like many other reef fishes, clownfish larvae have a suite of behaviors to affect their dispersal. Larval clownfish have strong swimming abilities upon hatching and can use olfactory, auditory, and visual cues to orient themselves as they swim in the ocean currents (Leis et al., 2011; Majoris et al., 2019).

We used empirical observations of dispersal in *A. clarkii* larvae measured with genetic mark–recapture data in Leyte, Philippines, during 2012–2014. Full methods are available in Catalano et al. (2021), but we combined North and South Magbangon into one site because both were within one grid cell of our oceanographic simulations. We therefore surveyed 18 reef patches along 30 km of coastline (Figure 1) and took samples of fish with a fork length greater than or equal to 3.5 cm. We genotyped 1244 individual fish at 1340 single nucleotide polymorphisms (SNPs) and used these genotypes to identify parent–offspring relationships for the 394 recruit-sized (standard length <6 cm) individuals (Catalano et al., 2021; Figure 1A).

### Biophysical connectivity simulations

We simulated larval dispersal by combining an oceanographic transport model with a dispersal model that

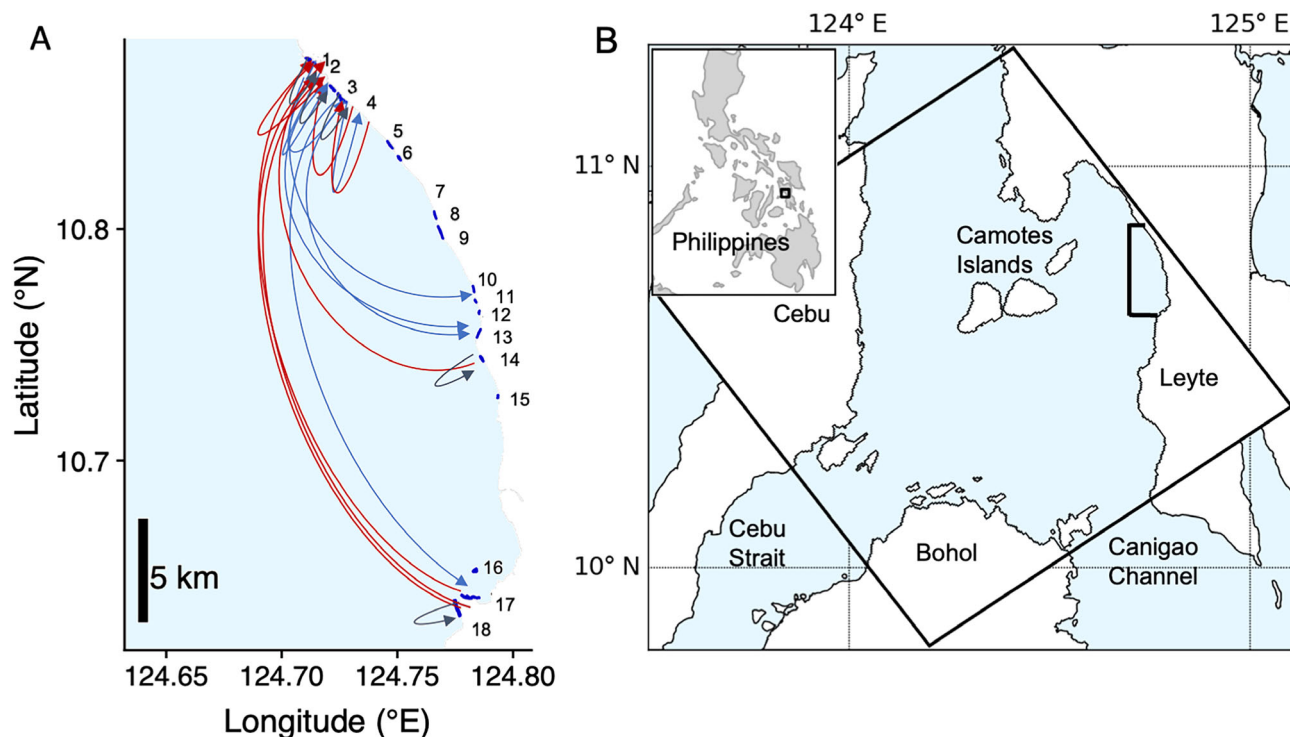


**FIGURE 1** (A) Map of the surveyed region in the Camotes Sea on the coast of Leyte, Philippines, with observed larval dispersal routes (red for northward, blue for southward, gray for self-recruitment). The 30-km coastline includes 18 habitat patches: Palanas (1), Wangag (2), Magbangon (3), Cabatoan (4), Caridad Cemetery (5), Caridad Proper (6), Hicgop South (7), Sitio Tugas (8), Elementary School (9), Sitio Lonas (10), San Agustin (11), Poroc San Flower (12), Poroc Rose (13), Visca (14), Gabas (15), Tomakin Dako (16), Haina (17), and Sitio Baybayon (18). (B) Camotes-ROMS model domain within the Philippines. The surveyed region of Leyte is bracketed in black. The western shore of Cebu and Sogod Bay in Leyte were not modeled and are therefore shown as land within the model domain.

accounted for spawning season, pelagic larval duration, and the spatial distribution of suitable habitat. We used a three-dimensional numerical model of oceanographic circulation, the Camotes Regional Ocean Modeling System (Figure 1, Camotes-ROMS). The model represents meso-scale and submesoscale physical oceanographic dynamics in response to heat flux, tidal mixing, and wind forcing with explicit topography (Haidvogel et al., 2008). Camotes-ROMS has a 500-m horizontal resolution with 50 terrain-following levels and bathymetry interpolated from SRTM30\_PLUS (Becker et al., 2009). Atmospheric conditions were from NASA's Modern-Era Retrospective Analysis (MERRA) (Rienecker et al., 2011) and open boundary conditions were from the extensively validated Coral Triangle ROMS simulations (CT-ROMS) (Castruccio et al., 2013). Tidal flows were imposed as tidal elevation and barotropic flows from the TPOX 8 Global Tidal Solutions model (Egbert & Erofeeva, 2002). We ran simulations from 2010 through 2015 with a 3-month spin-up in 2009 and saved output as daily averages. Camotes-ROMS temperatures compared favorably with ocean temperatures recorded adjacent to Visayas State University, with  $R^2$  values  $\geq 0.76$  (Appendix S1: Figure S1).

We calculated the average surface current velocity and average eddy kinetic energy (EKE) across the annual and monsoonal time periods to characterize oceanographic flow patterns. We calculated average daily surface current velocity from the daily average zonal (east–west) component of velocity  $u$  and meridional (north–south) velocity  $v$  for each grid cell:

$$c = \sqrt{u^2 + v^2}. \quad (1)$$

We then averaged the daily values for each year and for each multiannual monsoon season. EKE, or transient kinetic energy, measures ocean turbulence (including eddies), which is the dominant process countering transport by average currents on the timescales important to larval dispersal (Kang & Curchitser, 2017; Martínez-Moreno et al., 2019). For example, eddies and turbulence can help transport larvae against the mean current or retain them close to home (Byers & Pringle, 2006; Largier, 2003). We calculated the average EKE per unit mass for each grid cell using the daily surface current velocity components ( $u$  and  $v$ ) relative to the mean currents from January 1, 2010, to December 1, 2015 ( $\bar{u}$  and  $\bar{v}$ ):



$$\text{EKE} = \frac{u^2 + v^2}{2} - \frac{\bar{u}^2 + \bar{v}^2}{2}. \quad (2)$$

We then averaged the daily values of EKE for each year and the two multiannual monsoons.

We simulated passive (no behavior) larval dispersal using the offline Lagrangian particle tracking routine, TRACMASS (Döös et al., 2013). We released neutrally buoyant particles from the benthos of the focal patches. The model had background dissipation from the physics ( $10^{-5} \text{ m}^2 \text{ s}^{-1}$  background vertical mixing coefficient for momentum) but did not have explicit vertical dissipation for the particles. We also released particles from unsurveyed shallow (<10 m) reef habitat 10 km north and south of the surveyed area and all habitable reef around the three Camotes Islands. The Camotes are located 35 km offshore of the surveyed area (Figure 1). We released 1000 particles daily from each grid cell in the source reef areas from October to May to match *A. clarkii* reproduction (Holtswarth et al., 2017). Particles were recruited to the grid cell in which they were present on Day 8 post-release if that grid cell was a source patch. Parameters in this model were chosen based on the natural history of clownfish and were not tuned or fit to the observed genetic dispersal observations.

We use the term “recruitment” to describe the dispersal and settlement of a larva to suitable habitat in both the genetic observations and Lagrangian particle simulations for simplicity. However, these data differ in important ways. The particle simulations recreate hypothetical passive, oceanographically driven dispersal from the time of hatching to larval settlement at the end of the larval duration based on the principles of geophysical fluid dynamics. The field surveys sampled actual individuals that had dispersed, settled, recruited successfully on an anemone, and survived to the time of our sampling. Our genetic observations thus capture not only the environmental conditions representable in geophysical equations but also the full abiotic and biotic environmental and demographic influence of more behaviorally complex larvae and post-settlement survival, which are not modeled in our simulations. In other words, our simulations focus only on those mechanisms of oceanographic transport representable in circulation models.

## Likelihood-based model comparison

To test the contribution of oceanographic transport to observed connectivity variation, we compared observed and simulated connectivity matrices. We did not fit a

statistical model or estimate parameters for this comparison, but rather calculated the likelihood of the observations given the simulations. We grouped data on three timescales: across all 3 years (2012–2014) to create a multiannual average, by year to create annual averages, and by monsoon to create multiannual monsoon averages. We used *A. clarkii* growth rates to partition dispersal observations into time periods based on body size (Dedrick et al., 2021). Recruits were sampled in May and June and, if they measured less than 3.5 cm, were assumed to have dispersed between the preceding November and May (i.e., during the Amihan northeast monsoon season). In contrast, recruits greater than 4.5 cm but less than 6 cm were assumed to have dispersed between June and October during the preceding Habagat southwest monsoon season (Catalano et al., 2021). We constructed observed connectivity matrices  $B_t$  with elements  $b_{ijt}$  and rows  $i$  as source (parent) sites and columns  $j = 1 \dots S$  destination (recruit) sites for each time window  $t$  (Bode et al., 2019). The final row  $x$  of the matrix ( $b_{xjt}$ ) included sampled recruits without an identified parent, which is informative statistical information (Bode et al., 2018). We represented the simulation data as a connectivity matrix, with rows as source sites and columns as destination sites,  $M_t$  (see, e.g., Appendix S1: Figure S2).

We calculated the log-likelihood (Bode et al., 2019) of observing the parentage matrix  $B_t$  given a simulated connectivity matrix  $M_t$  with elements  $m_{ijt}$  as

$$\text{LL}(M_t|B_t) = \sum_{j=1}^S b_{xjt} \ln \left( \frac{\sum_{i=1}^S (1 - \pi_{it})^2 n_i \frac{m_{ijt}}{p_{it}}}{\sum_{a=1}^S n_a \frac{m_{ajt}}{p_{at}}} \right) + \sum_{i,j=1}^S b_{ijt} \ln \left( \frac{(1 - (1 - \pi_{it})^2) n_i \frac{m_{ijt}}{p_{it}}}{\sum_{a=1}^S n_a \frac{m_{ajt}}{p_{at}}} \right). \quad (3)$$

The function accounts for empirical sampling by incorporating population size at site  $i$  ( $n_i$ ) and the proportion of adults sampled at each site in each time period ( $\pi_{it}$ ), here given by the breeding female abundance (Appendix S1: Tables S1 and S2). The simulation connectivity matrix was normalized by the total number of particles released by each site  $i$  ( $p_{it}$ ) in time period  $t$ . The first term of the equation describes the log-likelihood of the unassigned recruits (no parent sampled) in the observed data, and the second term describes the log-likelihood of the assigned recruits (parentage assigned) in the observed data, given the particles recruiting along each simulated connectivity route.

We compared log-likelihoods across different combinations of observations and models. First, we calculated the log-likelihood of the observed multiannual (2012–2014) connectivity data conditional on the multiannual average

simulation data,  $LL(M_{2012-2014}|B_{2012}) + LL(M_{2012-2014}|B_{2013}) + LL(M_{2012-2014}|B_{2014})$ . We then compared this with the joint log-likelihood of the annual connectivity data conditional on the year-specific simulation data for each of the three years,  $LL(M_{2012}|B_{2012}) + LL(M_{2013}|B_{2013}) + LL(M_{2014}|B_{2014})$ . We also calculated McFadden's pseudo- $R^2$  (McFadden, 1977) as a measure of the goodness-of-fit increase from the multiannual average to the year-specific model ( $\text{pseudo-}R^2 = 1 - \frac{LL_{\text{year-specific}}}{LL_{\text{multi-annual average}}}$ ). Pseudo- $R^2$  values tend to be low, and values of 0.2–0.4 can be considered “excellent fit” (McFadden, 1977).

To test whether monsoonal oceanographic variation explained observed connectivity variation, we compared the log-likelihood of the observed connectivity matrix including only those recruits that could be partitioned into monsoon cohorts based on size at sampling conditional on the multiannual simulation connectivity data of the two monsoon seasons (Amihan, Amh, and Habagat, Hag) combined,  $LL(M_{\text{Amh} + \text{Hag}}|B_{\text{Amh}}) + LL(M_{\text{Amh} + \text{Hag}}|B_{\text{Hag}})$ , to the joint log-likelihood of the monsoonal connectivity data conditional on the simulation data specific to each of the two monsoon seasons Amihan and Habagat,  $LL(M_{\text{Amh}}|B_{\text{Amh}}) + LL(M_{\text{Hag}}|B_{\text{Hag}})$ .

To account for uncertainty, we resampled both the observed *A. clarkii* recruitment events ( $n = 394$  juveniles, whether matched to parents or not) and the simulated recruitment events (955,263 particles that recruited back to the source reefs) 1000 times with replacement. The simulations recreated many dispersal events, while our observations sampled much less extensively. To account for uncertainty created by limited sampling, we also downsampled our simulations by resampling 394 individual recruits with replacement from the simulation data according to the actual number of individual recruits sampled at each site in each year (Appendix S1: Table S2). We repeated this procedure 1000 times. We then applied the likelihood function to each resampled iteration of observed, simulated, and downsampled simulation connectivity matrices.

## Comparing simulated and observed dispersal

We tested how well the simulation recreated the observed spatial scale of dispersal and the magnitude of dispersal variation across timescales. To do so, we fit generalized Gaussian dispersal kernels to the observed and simulated data (Bode et al., 2018; Catalano et al., 2021). The dispersal kernel was an isotropic probability density function that described dispersal ( $p$ ) from the natal patch  $i$  to patch  $j$  with distance ( $d$ ) as:

$$p(k, \theta, d_{ij}) = \frac{e^{k\theta}}{\Gamma(\frac{1}{\theta})} e^{-(e^{k\theta} d_{ij})^\theta}, \quad (4)$$

where  $\Gamma$  denotes the gamma function (Bode et al., 2018). We used maximum likelihood optimization in R version 3.6.1 with the package *bbmle* (Bolker et al., 2017; R Core Team, 2019) to estimate the scale parameter  $k$  (dispersion) and a shape parameter  $\theta$  (kurtosis) that affects how much of the density is contained in the tail (Catalano et al., 2021).

We fit dispersal kernels to the simulation data and genetic observations of dispersal grouped on multiannual (2012–2014), annual, and monsoonal timescales. We then used the kernels to calculate unsigned mean dispersal distance, a common measure of the spatial scale of dispersal. To account for uncertainty, we calculated distance from each of the resampled connection matrices ( $n = 1000$ ) described in the previous section. To compare the magnitude of temporal variation in mean dispersal distance between the observations and simulations, we calculated the mean dispersal distance CV (equal to the SD divided by the mean) across years and across monsoons, plus uncertainty in these calculations across each bootstrapped iteration.

## RESULTS

### Camotes-ROMS circulation

Along the coast of Leyte on the eastern edge of the Camotes Sea, currents flow predominantly southward alongshore (Figure 2). The greatest average current speed and EKE across sites was in 2013 (Figures 2 and 3; Appendix S1: Figures S3 and S4, Table S3). The average alongshore current speed across the sites was greatest during the Habagat southwest monsoon (June–October), although the northernmost sites experienced greater current speeds during the Amihan northeast monsoon (November through May, Appendix S1: Figure S3). There was no major monsoon-driven current reversal in this nearshore area (Figure 2A,B). The EKE was generally greater during Amihan (Figure 3A,B; Appendix S1: Figure S4, Table S3). Overall, the average currents and EKE generally differed more between monsoons (for which wind directions differ substantially) than across years.

### Likelihood-based model comparison

The model comparison demonstrated that the interannually varying biophysical simulations, rather than

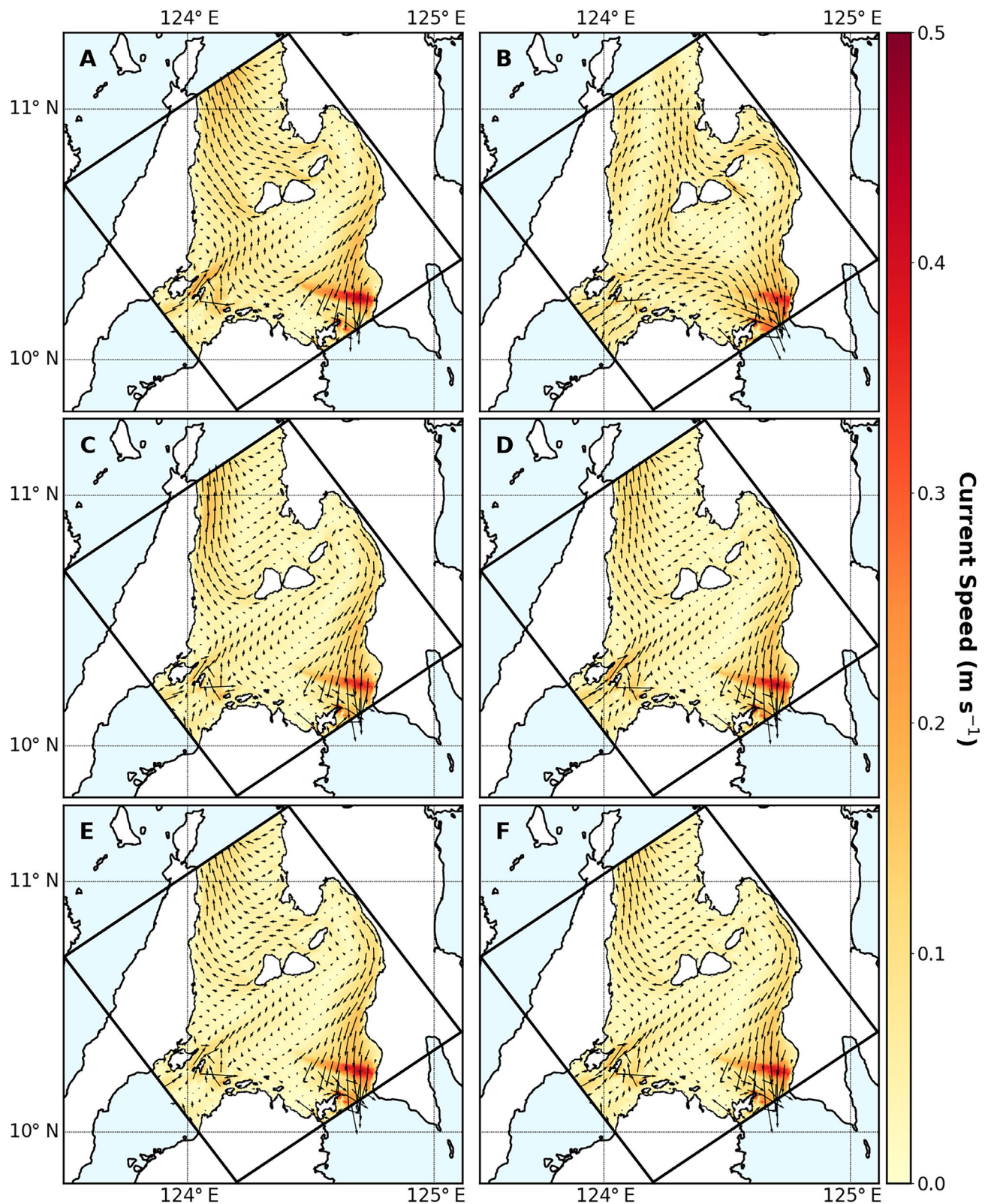


**FIGURE 2** Average surface current speed (in meters per second) during the Amihan northeast monsoon season (A) and the Habagat southwest monsoon season (B); for the years 2012 (C), 2013 (D), and 2014 (E); and the average for 2012–2014 (F).

the average connectivity patterns, produced a higher likelihood of the observed connectivity data (Figure 4). In other words, the biophysical simulations accurately

represented interannual variability that was relevant for larval dispersal. Sites further south in the study region contributed, in particular, to the better



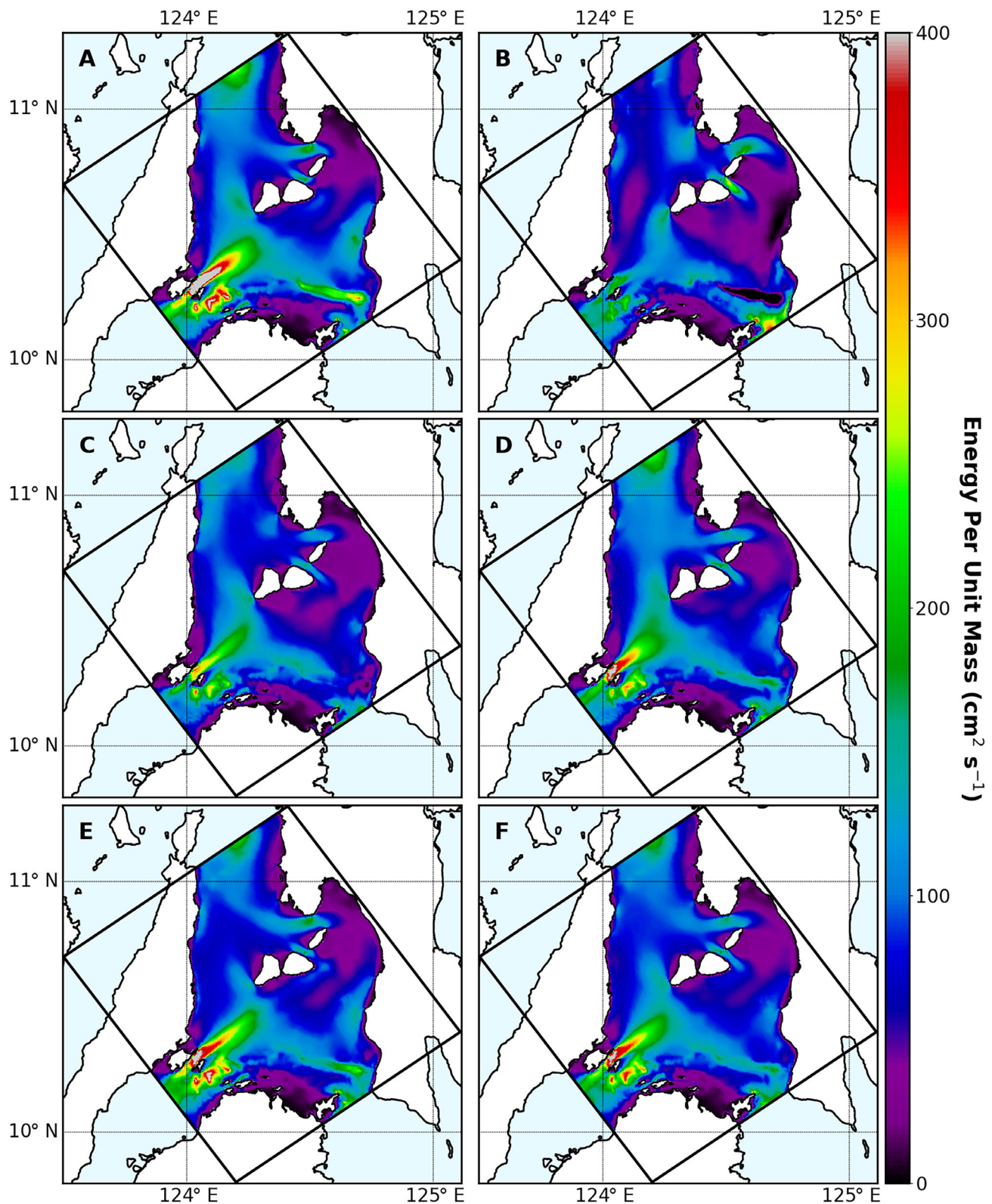


**FIGURE 3** Average eddy kinetic energy per unit mass (in square centimeters per second) during the Amihan northeast monsoon (A) and the Habagat southwest monsoon (B); for the years 2012 (C), 2013 (D), and 2014 (E); and the average for 2012–2014 (F).

performance of interannual simulations (Appendix S1: Figure S5). The pseudo- $R^2$  value was 0.128. In addition, the likelihood was greatest when using the

simulation data downsampled according to the empirical sampling scheme and the pseudo- $R^2$  value increased to 0.405, suggesting that additional variability



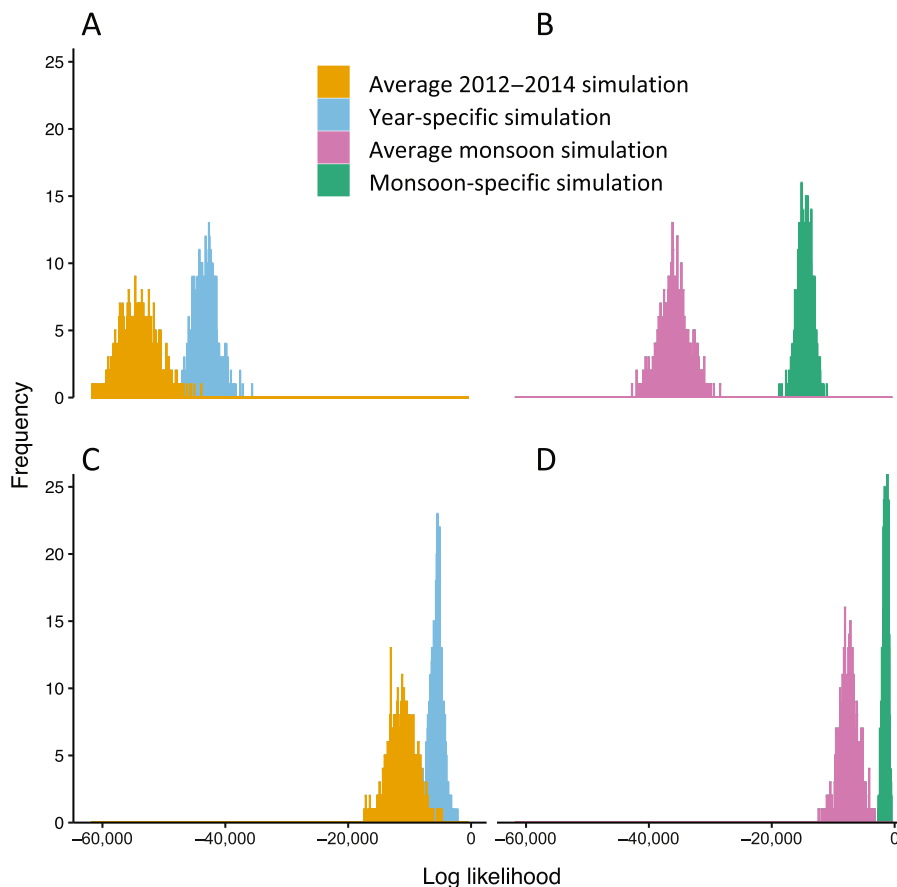


**FIGURE 4** Log-likelihood distributions of the (A and C) year-specific and 2012–2014 average simulation matrices, and (B and D) monsoon-specific and cross-monsoon average simulation matrices. In (A and B), the simulation matrices include all simulated particles. In (C and D), the simulated matrices were downsampled to match the observation sample sizes.

in the observations was caused by the sampling process (Figure 4A,C).

Similarly, the monsoon-specific simulations had higher likelihood than the cross-monsoon average simulations (Figure 4B), and the likelihood was higher when the simulation data were downsampled than when they were not (Figure 4B,D). The pseudo- $R^2$  value increased from 0.433 without downsampling to 0.775 with downsampling.

### Comparing simulated and observed scales of dispersal

The dispersal simulations consistently predicted smaller spatial scales of dispersal than those observed (Figure 5; Appendix S1: Figure S6). For example, the mean dispersal distance calculated from the aggregate observed dispersal kernel for 2012–2014 (13.7 km with 95% CI of 10.5–18.5) was greater than that from the simulated kernel (3.77 km with 95% CI of 3.76–3.77) (Figure 5; Appendix S1: Figure S6, Table S4). However, the simulations did capture

greater mean dispersal distance during Habagat than during Amihan (Figure 5; Appendix S1: Figure S6, Table S4), matching the greater simulated current speeds during Habagat (Figure 2; Appendix S1: Figure S3, Table S3).

There was some correspondence in shape between the observed and simulated kernels. For example, the 2014, 2012–2014, and Amihan kernels were leptokurtic (i.e., more outliers than a Gaussian distribution;  $\theta < 1$ ) for both the observations and the simulations (Figure 5; Appendix S1: Figure S7, Table S4). However, the observed 2012, 2013, and Habagat kernels were platykurtic (i.e., fewer outliers;  $\theta > 1$ ), while the simulated kernels were leptokurtic (Figure 5; Appendix S1: Figure S7, Table S4).

Interannual variation in mean dispersal was greater in the observations (median CV 1.04) than expected from the simulations (0.08, Figure 6). Downsampling the simulations produced interannual variation (median CV 0.22) somewhat closer to that observed (Figure 6). In contrast, the observed monsoonal variation (0.31) was comparable to the simulated variation (0.39, Figure 6). Downsampling reduced the expected monsoonal variation (Figure 6, median CV 0.03).

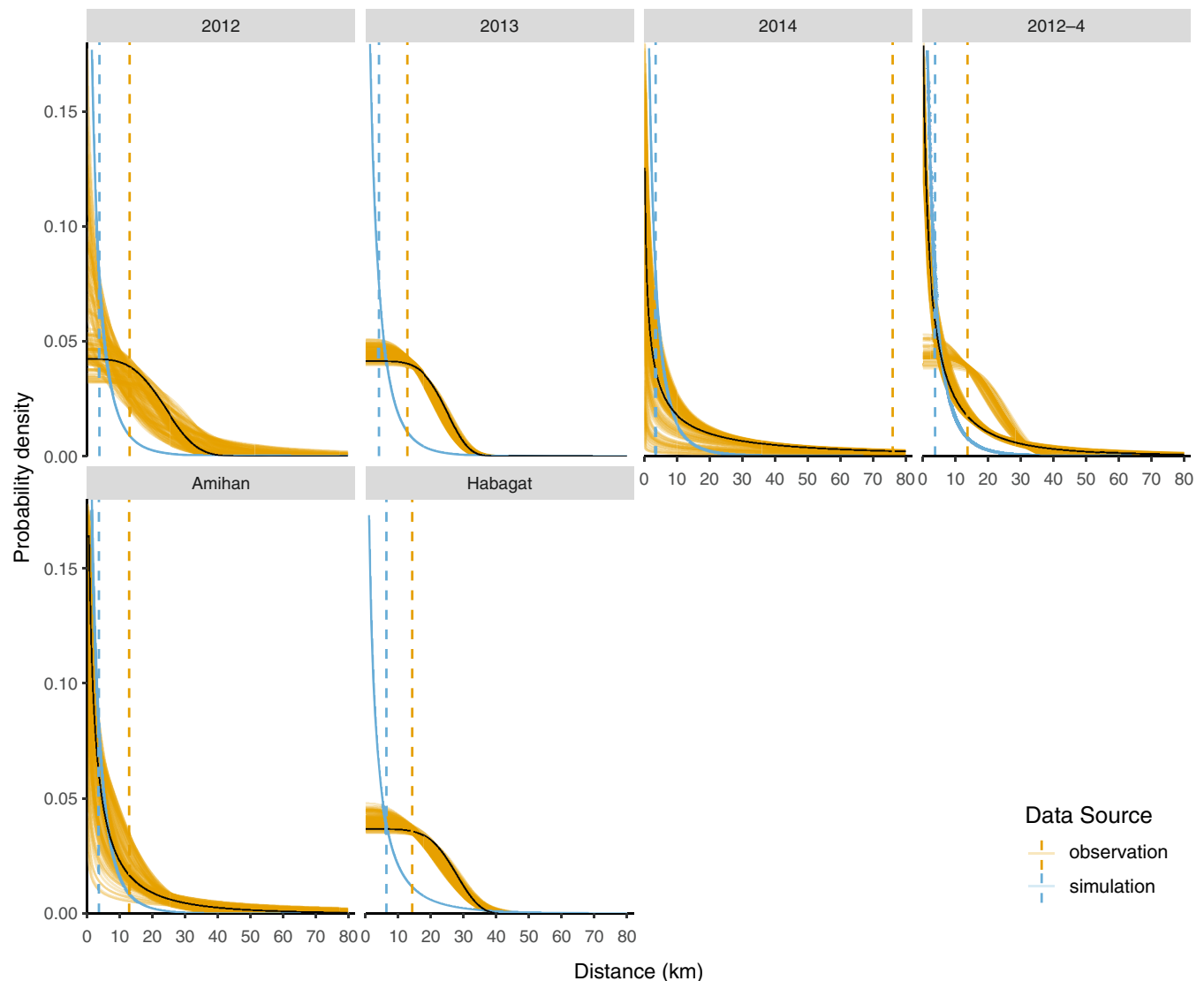


**FIGURE 5** Dispersal kernels fit to genetic parentage observations (orange) and to biophysical simulations (blue) on annual, monsoonal, and aggregate timescales (2012–2014). Figure shows best-fit kernel for the observations (solid black line), 100 kernels drawn from the log-likelihood profiles (colored lines), and mean dispersal distances (dashed vertical lines).

## DISCUSSION

Despite ample observation that dispersal patterns vary through time, it has been substantially more difficult to understand the extent to which environmental variability explains variation in larval connectivity. Mechanistic studies of dispersal have the power to illuminate the factors shaping connectivity patterns across time. Here, we showed that temporal variation in nearshore oceanographic transport is a key mechanism structuring annual and seasonal dispersal of the coral reef fish *A. clarkii*. We found that biophysical simulations of the nearshore environment explained interannual and monsoonal variation in observed dispersal, although the simulations consistently underestimated the spatial scale of dispersal and

the magnitude of dispersal variation among years. Our results empirically demonstrate that variation in near-shore oceanographic flow contributes to the emergent variation in larval dispersal.

We found that the observed dispersal patterns were better explained by interannually varying ocean currents, rather than average ocean currents, supporting our hypothesis that variability in oceanographic transport contributes to interannual variation in larval dispersal. This finding was not a foregone conclusion, because oceanographic models often have difficulty representing mesoscale currents in time and space, particularly in data-limited regions of the world, and average statistical distributions are often more appropriate (Edwards et al., 2015). This finding using mechanistic, biophysical

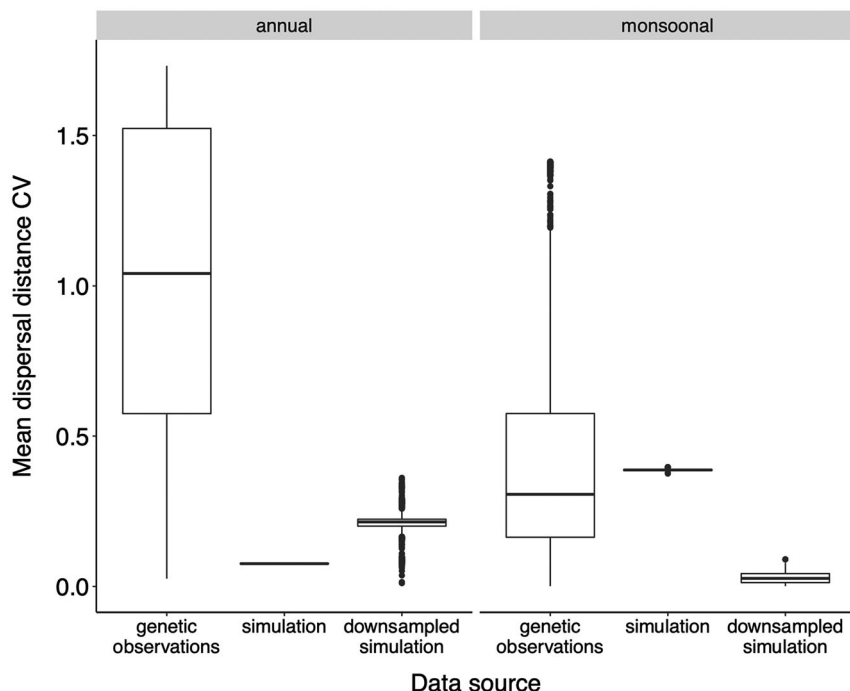


**FIGURE 6** CV in mean dispersal distance for bootstrapped observations, simulations, and downsampled simulation dispersal kernels across years and monsoons.

models of larval dispersal extends previous associations between current directions and dispersal in other near-shore marine taxa (Abesamis et al., 2017; Carson et al., 2010). This annual variation in current speed may in part be driven by annual variation in monsoon activity. The timing of Habagat onset (southwest monsoon, which has more advection than the Amihan northeast monsoon) can be anywhere from early May to early July, resulting in years with an earlier onset experiencing a longer Habagat monsoon season. The timing of Habagat onset depends on the initiating atmospheric factors like the arrival of warm and moist air from tropical cyclones (Kubota et al., 2017). Annual circulation differences caused by Habagat onset variation could also be affected by sea surface temperature anomalies from the El Niño Southern Oscillation (ENSO). In our eastern Camotes Sea simulations, the shortest annual mean dispersal distance was in 2014, following a weak El Niño event in 2013 and consistent with observations of decreased Habagat activity following El Niño events (Xie et al., 2009). Further investigation of these and related climate mechanisms will require more than the three-year time series we had available because these environmental phenomena operate on longer time periods and require more observations to understand the range of potential impacts on connectivity. Even so, these results empirically support the hypothesis that annual variation in oceanographic transport contributes to annual variation in emergent

connectivity, and that mechanistic biophysical models accurately represent this variation (Mitarai et al., 2008; Siegel et al., 2008).

The biophysical simulations demonstrated substantial variation in ocean currents between monsoon seasons and predicted a greater spatial scale of dispersal during Habagat that was also apparent in the empirical dispersal observations. In the eastern Camotes Sea, currents flow southward along the coast of Leyte in both monsoons but strengthen during Habagat, consistent with the observations of greater mean dispersal distances during Habagat. EKE was also lower during Habagat, suggesting that stronger eddy activity contributes to larval retention and does not contribute to extensive larval dispersal. Along the coast of the nearby island of Negros in the Philippines, the reef fish *Chaetodon vagabundus* disperses predominantly northeastward during Habagat and southwestward during Amihan, coincident with the prevailing wind direction of each monsoon and supporting the idea that monsoonal variation in dispersal is driven by changing oceanographic transport (Abesamis et al., 2017). Our coincident observations and simulations further demonstrated that monsoonal variation in oceanographic transport is a key mechanism driving monsoonal variation in connectivity.

One notable finding was the generally shorter scales of simulated dispersal than the scales observed. Several aspects of the numerical models could have contributed



to reduced dispersal. First, the atmospheric forcing conditions prescribed by MERRA are coarser resolution ( $\frac{1}{2}^\circ$  latitude  $\times$   $\frac{2}{3}^\circ$  longitude; Rienecker et al., 2011) than the Camotes-ROMS (500 m) by roughly two orders of magnitude. While these forcing conditions provide a reasonable estimate of the broadscale atmospheric state, they omit localized processes that could alter ocean currents and eddies. Second, TRACMASS was run offline using daily average values for ocean currents, which underrepresents diurnal variation in currents (e.g., tides and weather). TRACMASS was also run without the addition of numerical diffusion: particles were seeded within grid cells in a spatially even, rectangular configuration. This approach sampled a range of linearly interpolated velocity fields in the ocean grid cell but did not reproduce fluid diffusion or turbulence. Lastly, we seeded 1000 particles per grid cell to keep computation time lower, but this number may not fully represent potential dispersal (Brickman & Smith, 2002; Simons et al., 2013).

Our simulations were designed to isolate the effect of oceanographic transport and did not include any larval behaviors that would allow individuals to modify their movement (Burgess et al., 2022; Leis et al., 2011; Majoris et al., 2019; Nanninga & Manica, 2018). Along with physical processes not fully captured by the simulations, the lack of larval behavior likely contributed to some of the differences between observations and simulations, including the smaller scale of simulated dispersal distances than those observed. Larvae exhibit swimming abilities that increase throughout development, and orientation abilities that help them choose a position in the water column and navigate toward suitable habitat (Fisher, 2005; Lecchini et al., 2005; Leis et al., 2011; Simpson et al., 2010). For example, damselfish larvae in the Caribbean can actively move below the wind-driven surface layer and mitigate advection away from suitable habitat in the nearshore environment (Paris et al., 2007; Paris & Cowen, 2004). Studies of *P. maculatus* connectivity in the Great Barrier Reef system demonstrate that adding larval behaviors like ontogenetic vertical migration, swimming performance, and orientation in biophysical simulations enhances the correspondence between simulations and observations, relative to passive simulations (Bode et al., 2019).

For fast swimming larvae like *A. clarkii*, we hypothesize that incorporating larval swimming and orientation in simulations will increase larval diffusion and enhance the probability of settlement, thereby increasing the predicted mean dispersal distance (Burgess et al., 2022). This hypothesis is contrary to expectations from research in other marine systems, which suggests larvae use their swimming abilities to stay close to their natal locations (Fobert et al., 2019; Paris et al., 2007). However,

swimming is also used by larvae while feeding and finding suitable settlement habitat, not simply navigating to their natal reef. Feeding movements may increase diffusion and therefore increase dispersal away from natal sites. In addition, swimming to suitable habitats can increase the settlement success of even long-distance dispersers (Burgess et al., 2022; Nanninga & Manica, 2018). Meta-analyses demonstrate that swimming ability is a good proxy for reef fish dispersal capacity and is correlated with greater gene flow and range size (Majoris et al., 2019; Nanninga & Manica, 2018). Our comparison of empirical observations with passive simulations highlights the complex relationship between larval behavior and oceanographic transport and contributes to a broader effort to understand this interaction.

Our observations of mean dispersal distance demonstrated much stronger annual variation than the biophysical simulations, but monsoonal variation was comparable between observations and simulations. Some of this disparity in annual estimates was explained by subsampling the simulations to replicate our sampling effort in the field, revealing that some, but not all, of the excess interannual variation was from sampling variance. In addition, biological processes such as reproduction and survival may explain the remainder of the unexplained variation on annual timescales. For example, in coastal kelp forests, annual variation in connectivity is driven by an interaction between temporal variation in fecundity and dispersal (Castorani et al., 2017). Fecundity variation could interact with spatial dispersal heterogeneity in *A. clarkii*, such that different sites with different dispersal potentials have greater or lesser reproductive success each year, leading to higher levels of dispersal along some routes relative to other routes in a given year. Additionally, an individual's dispersal history can have important implications for post-settlement survival, such that larvae along certain trajectories are more likely to survive in a given year (Hamilton et al., 2008). *A. clarkii* survival post-recruitment is also influenced by predation, other biotic interactions, and temperature, and warmer temperatures enhance survival markedly when compared with cooler temperatures (Le et al., 2011). Temperature anomalies in a given year are likely more pronounced at shallower sites, disproportionately increasing or decreasing the relative number of dispersing and surviving individuals observed along routes to shallow settlement sites. This effect would influence our observations of post-recruitment individuals, but not our simulations because the latter did not include survival. Our monsoonal estimates were multiannual averages of connectivity, and this may explain why accounting for the sampling process introduced less variability than it did on annual timescales. Taken together, variation in larval

connectivity results from a sequence of biotic and abiotic processes that are heterogeneous across both time and space in many coastal systems, including but not limited to physical transport.

Our results demonstrate the ability of high-resolution biophysical simulations to predict some of the observed temporal variation in larval connectivity, but they are only a first step toward understanding the mechanisms of connectivity variation. Research that includes larval behavior in biophysical simulations will help reveal the relative contribution and possible interactions of larval behavior and oceanographic forcing in a hypothesis testing framework. Further investigation into the contribution of environmental stochasticity to connectivity variation is needed in diverse systems and across longer timescales to identify the effects of phenomena like decadal atmospheric oscillations. As future work continues to characterize the mechanisms of variability that can be incorporated in biophysical models, it will become possible to elucidate how dispersal variation affects emergent processes such as local adaptation and population persistence, enabling further research with a tractable modeling framework to complement extensive empirical surveys.

Dispersal is central to ecological and evolutionary processes, from population and community dynamics to local adaptation (da Silva Carvalho et al., 2015; Hastings & Botsford, 2006; Resasco & Fletcher, 2021; Tigano & Friesen, 2016). Temporal variation in dispersal may enhance or diminish population persistence, drive community turnover and range expansions, and contribute to temporal heterogeneity in genetic structure (Harrison et al., 2020; Klein et al., 2016; Matias et al., 2013). The mechanistic understanding developed here demonstrates the power of concurrent empirical and simulation-based analysis to illuminate the long-standing “black box” of larval dispersal in connectivity science (Counsell et al., 2022; Cowen, 2002).

## AUTHOR CONTRIBUTIONS

Katrina A. Catalano and Malin L. Pinsky conceptualized the project. Katrina A. Catalano, Elizabeth J. Drenkard, Enrique N. Curchitser, Allison G. Dedrick, and Malin L. Pinsky developed the methodology. Katrina A. Catalano, Elizabeth J. Drenkard, and Allison G. Dedrick managed the software. Katrina A. Catalano conducted the formal analysis. Katrina A. Catalano, Michelle R. Stuart, Humberto R. Montes, Jr., and Malin L. Pinsky performed the investigation. Enrique N. Curchitser and Humberto R. Montes, Jr. provided the resources. Katrina A. Catalano, Michelle R. Stuart, and Malin L. Pinsky handled data curation. Katrina A. Catalano wrote the original draft. Katrina A. Catalano, Elizabeth J. Drenkard, Enrique N. Curchitser, and Malin L. Pinsky were responsible for

writing, review, and editing. Katrina A. Catalano, Elizabeth J. Drenkard, and Malin L. Pinsky managed the visualization. Malin L. Pinsky supervised the project. Michelle R. Stuart and Malin L. Pinsky oversaw project administration. Enrique N. Curchitser and Malin L. Pinsky acquired the funding.

## ACKNOWLEDGMENTS

We thank Visayas State University and the municipalities of Baybay City and Albura for field support. We thank Geralde Sucano, Beverlito Montalban, Teresita Idara, Rogello Nicanor, Liza Espinosa, Noel Alquino, Carlos Balansuna, Froilan Beñas, Danilo Marine, and Arturo Bastasa for field assistance. We thank Charles Stock and John Dunne for comments on an earlier draft. Funding was provided by an Alfred P. Sloan Foundation Fellowship No. BR2014-044; an Oak Ridge Associated Universities (ORAU) Ralph E. Powe Junior Faculty Enhancement award; National Science Foundation award Nos. OCE-1426891, OCE-1430218, and OISE-1743711; and Rutgers University.

## CONFLICT OF INTEREST STATEMENT

The authors declare no conflicts of interest.

## DATA AVAILABILITY STATEMENT

Data and code (Catalano & Pinsky, 2024) are available in Zenodo at <https://doi.org/10.5281/zenodo.12744525>. Surface current data (Pinsky et al., 2023) are available in figshare at <https://doi.org/10.6084/m9.figshare.22827059.v1>.

## ORCID

Malin L. Pinsky  <https://orcid.org/0000-0002-8523-8952>

## REFERENCES

- Abesamis, R. A., P. Saenz-Agudelo, M. L. Berumen, M. Bode, C. R. L. Jadloc, L. A. Solera, C. L. Villanoy, L. P. C. Bernardo, A. C. Alcala, and G. R. Russ. 2017. “Reef-Fish Larval Dispersal Patterns Validate No-Take Marine Reserve Network Connectivity that Links Human Communities.” *Coral Reefs* 36: 791–801.
- Bani, R., M.-J. Fortin, R. M. Daigle, and F. Guichard. 2019. “Dispersal Traits Interact with Dynamic Connectivity to Affect Metapopulation Growth and Stability.” *Theoretical Ecology* 12: 111–127.
- Becker, J. J., D. T. Sandwell, W. H. F. Smith, J. Braud, B. Binder, J. Depner, D. Fabre, et al. 2009. “Global Bathymetry and Elevation Data at 30 Arc Seconds Resolution: SRTM30\_PLUS.” *Marine Geodesy* 32: 355–371.
- Berumen, M. L., G. R. Almany, S. Planes, G. P. Jones, P. Saenz-Agudelo, and S. R. Thorrold. 2012. “Persistence of Self-Recruitment and Patterns of Larval Connectivity in a Marine Protected Area Network.” *Ecology and Evolution* 2: 444–452.
- Bode, M., J. M. Leis, L. B. Mason, D. H. Williamson, H. B. Harrison, S. Choukroun, and G. P. Jones. 2019. “Successful Validation of

- a Larval Dispersal Model Using Genetic Parentage Data.” *PLoS Biology* 17: e3000380.
- Bode, M., D. H. Williamson, H. B. Harrison, N. Outram, and G. P. Jones. 2018. “Estimating Dispersal Kernels Using Genetic Parentage Data.” *Methods in Ecology and Evolution* 9: 490–501.
- Bolker, B., R Development Core Team, and I. Giné-Vázquez. 2017. “bblme: Tools for General Maximum Likelihood Estimation.” <https://CRAN.R-project.org/package=bblme>.
- Brickman, D., and P. C. Smith. 2002. “Lagrangian Stochastic Modeling in Coastal Oceanography.” *Journal of Atmospheric and Oceanic Technology* 19: 83–99.
- Burgess, S. C., M. Bode, J. M. Leis, and L. B. Mason. 2022. “Individual Variation in Marine Larval-Fish Swimming Speed and the Emergence of Dispersal Kernels.” *Oikos* 2022: 2022.
- Burgess, S. C., K. J. Nickols, C. D. Griesemer, L. A. K. Barnett, A. G. Dedrick, E. V. Satterthwaite, L. Yamane, S. G. Morgan, J. W. White, and L. W. Botsford. 2014. “Beyond Connectivity: How Empirical Methods Can Quantify Population Persistence to Improve Marine Protected-Area Design.” *Ecological Applications* 24: 257–270.
- Byers, J. E., and J. M. Pringle. 2006. “Going against the Flow: Retention, Range Limits and Invasions in Advective Environments.” *Marine Ecology Progress Series* 313: 27–41.
- Carson, H. S., P. C. López-Duarte, L. L. Rasmussen, D. Wang, and L. A. Levin. 2010. “Reproductive Timing Alters Population Connectivity in Marine Metapopulations.” *Current Biology* 20: 1926–31.
- Castorani, M. C. N., D. C. Reed, P. T. Raimondi, F. A. Alberto, T. W. Bell, K. C. Cavanaugh, D. A. Siegel, and R. D. Simons. 2017. “Fluctuations in Population Fecundity Drive Variation in Demographic Connectivity and Metapopulation Dynamics.” *Proceedings of the Royal Society of London B: Biological Sciences* 284(1847): 20162086.
- Castruccio, F. S., E. N. Curchitser, and J. A. Kleypas. 2013. “A Model for Quantifying Oceanic Transport and Mesoscale Variability in the Coral Triangle of the Indonesian/Philippines Archipelago.” *Journal of Geophysical Research: Oceans* 118: 6123–44.
- Catalano, K. A., A. G. Dedrick, M. R. Stuart, J. B. Puritz, H. R. Montes, and M. L. Pinsky. 2021. “Quantifying Dispersal Variability among Nearshore Marine Populations.” *Molecular Ecology* 30: 2366–77.
- Catalano, K. A., and M. L. Pinsky. 2024. “CamotesROMS Code (v1.0).” Zenodo. <https://doi.org/10.5281/zenodo.12744526>.
- Counsell, C. W. W., R. R. Coleman, S. S. Lal, B. W. Bowen, E. E. Franklin, A. B. Neuheimer, B. S. Powell, et al. 2022. “Interdisciplinary Analysis of Larval Dispersal for a Coral Reef Fish: Opening the Black Box.” *Marine Ecology Progress Series* 684: 117–132.
- Cowen, R. K. 2002. “Larval Dispersal and Retention and Consequences for Population Connectivity.” In *Coral Reef Fishes: Dynamics and Diversity in a Complex Ecosystem*, edited by P. F. Sale, 149–170. San Diego, CA: Academic Press.
- Cowen, R. K., and S. Sponaugle. 2009. “Larval Dispersal and Marine Population Connectivity.” *Annual Review of Marine Science* 1: 443–466.
- da Silva Carvalho, C., M. C. Ribeiro, M. C. Côrtes, M. Galetti, and R. G. Collevatti. 2015. “Contemporary and Historic Factors Influence Differently Genetic Differentiation and Diversity in a Tropical Palm.” *Heredity* 115: 216–224.
- Dedrick, A. G., K. A. Catalano, M. R. Stuart, J. W. White, H. R. Montes, and M. L. Pinsky. 2021. “Persistence of a Reef Fish Metapopulation Via Network Connectivity: Theory and Data.” *Ecology Letters* 24: 1121–32.
- Döös, K., J. Kjellsson, and B. Jönsson. 2013. “TRACMASS—A Lagrangian Trajectory Model.” In *Preventive Methods for Coastal Protection*, edited by T. Soomere and E. Quak, 225–249. Heidelberg: Springer International Publishing.
- Edwards, C. A., A. M. Moore, I. Hoteit, and B. D. Cornuelle. 2015. “Regional Ocean Data Assimilation.” *Annual Review of Marine Science* 7: 21–42.
- Egbert, G. D., and S. Y. Erofeeva. 2002. “Efficient Inverse Modeling of Barotropic Ocean Tides.” *Journal of Atmospheric and Oceanic Technology* 19: 183–204.
- Fisher, R. 2005. “Swimming Speeds of Larval Coral Reef Fishes: Impacts on Self-Recruitment and Dispersal.” *Marine Ecology Progress Series* 285: 223–232.
- Fobert, E. K., E. A. Trembl, and S. E. Swearer. 2019. “Dispersal and Population Connectivity Are Phenotype Dependent in a Marine Metapopulation.” *Proceedings of the Royal Society B: Biological Sciences* 286: 20191104.
- Gaines, S. D., and M. D. Bertness. 1992. “Dispersal of Juveniles and Variable Recruitment in Sessile Marine Species.” *Nature* 360: 579–580.
- Gilg, M. R., and T. J. Hilbish. 2003. “The Geography of Marine Larval Dispersal: Coupling Genetics with Fine-Scale Physical Oceanography.” *Ecology* 84: 2989–98.
- Haidvogel, D. B., H. Arango, W. P. Budgell, B. D. Cornuelle, E. Curchitser, E. Di Lorenzo, K. Fennel, et al. 2008. “Ocean Forecasting in Terrain-Following Coordinates: Formulation and Skill Assessment of the Regional Ocean Modeling System.” *Journal of Computational Physics* 227: 3595–3624.
- Hamilton, S. L., J. Regetz, and R. R. Warner. 2008. “Postsettlement Survival Linked to Larval Life in a Marine Fish.” *Proceedings of the National Academy of Sciences of the United States of America* 105: 1561–66.
- Harrison, H. B., M. Bode, D. H. Williamson, M. L. Berumen, and G. P. Jones. 2020. “A Connectivity Portfolio Effect Stabilizes Marine Reserve Performance.” *Proceedings of the National Academy of Sciences of the United States of America* 117(25595–25): 600.
- Hastings, A., and L. W. Botsford. 2006. “Persistence of Spatial Populations Depends on Returning Home.” *Proceedings of the National Academy of Sciences of the United States of America* 103: 6067–72.
- Hogan, J. D., R. J. Thiessen, P. F. Sale, and D. D. Heath. 2012. “Local Retention, Dispersal and Fluctuating Connectivity among Populations of a Coral Reef Fish.” *Oecologia* 168: 61–71.
- Holtswarth, J. N., S. B. San Jose, H. R. Montes, Jr., J. W. Morley, and M. L. Pinsky. 2017. “The Reproductive Seasonality and Fecundity of Yellowtail Clownfish (*Amphiprion clarkii*) in The Philippines.” *Bulletin of Marine Science* 93: 997–1007.
- Kang, D., and E. N. Curchitser. 2017. “On the Evaluation of Seasonal Variability of the Ocean Kinetic Energy.” *Journal of Physical Oceanography* 47: 1675–83.
- Klein, M., S. Teixeira, J. Assis, E. A. Serrão, E. J. Gonçalves, and R. Borges. 2016. “High Interannual Variability in Connectivity



- and Genetic Pool of a Temperate Clingfish Matches Oceanographic Transport Predictions." *PLoS One* 11: e0165881.
- Kubota, H., R. Shirooka, J. Matsumoto, E. O. Cayan, and F. D. Hilario. 2017. "Tropical Cyclone Influence on the Long-Term Variability of Philippine Summer Monsoon Onset." *Progress in Earth and Planetary Science* 4: 27.
- Largier, J. L. 2003. "Considerations in Estimating Larval Dispersal Distances from Oceanographic Data." *Ecological Applications* 13: S71–S89.
- Lau, K. M., and S. Yang. 1997. "Climatology and Interannual Variability of the Southeast Asian Summer Monsoon." *Advances in Atmospheric Sciences* 14: 141–162.
- Le, Y., Y. Sheng-Yun, Z. Xiao-Ming, L. Min, L. Jing-Yi, and W. Kai-Chang. 2011. "Effects of Temperature on Survival, Development, Growth and Feeding of Larvae of Yellowtail Clownfish *Amphiprion clarkii* (Pisces: Perciformes)." *Acta Ecologica Sinica* 31: 241–45.
- Lecchini, D., J. Shima, B. Banaigs, and R. Galzin. 2005. "Larval Sensory Abilities and Mechanisms of Habitat Selection of a Coral Reef Fish during Settlement." *Oecologia* 143: 326–334.
- Leis, J. M., U. E. Siebeck, and D. L. Dixon. 2011. "How Nemo Finds Home: The Neuroecology of Dispersal and of Population Connectivity in Larvae of Marine Fishes." *Integrative and comparative biology* 51: 826–843.
- Majoris, J. E., K. A. Catalano, D. Scolaro, J. Atema, and P. M. Buston. 2019. "Ontogeny of Larval Swimming Abilities in Three Species of Coral Reef Fishes and a Hypothesis for Their Impact on the Spatial Scale of Dispersal." *Marine Biology* 166: 159.
- Martínez-Moreno, J., A. M. Hogg, A. E. Kiss, N. C. Constantinou, and A. K. Morrison. 2019. "Kinetic Energy of Eddy-Like Features from Sea Surface Altimetry." *Journal of Advances in Modeling Earth Systems* 11: 3090–3105.
- Matias, M. G., N. Mouquet, and J. M. Chase. 2013. "Dispersal Stochasticity Mediates Species Richness in Source-Sink Metacommunities." *Oikos* 122: 395–402.
- McFadden, D. 1977. *Quantitative Methods for Analyzing Travel Behavior of Individuals: Some Recent Developments*. Cowles Foundation Discussion Paper No. 474. 1–48. New Haven, CT: Cowles Foundation for Research in Economics at Yale University.
- Mitarai, S., D. A. Siegel, and K. B. Winters. 2008. "A Numerical Study of Stochastic Larval Settlement in the California Current System." *Journal of Marine Systems* 69: 295–309.
- Moyer, J. T. 1986. "Longevity of the Anemonefish *Amphiprion clarkii* at Miyake-Jima, Japan with Notes on Four Other Species." *Copeia* 1986: 135–39.
- Nanninga, G. B., and A. Manica. 2018. "Larval Swimming Capacities Affect Genetic Differentiation and Range Size in Demersal Marine Fishes." *Marine Ecology Progress Series* 589: 1–12.
- Ochi, H. 1986. "Growth of the Anemonefish *Amphiprion clarkii* in Temperate Waters, with Special Reference to the Influence of Settling Time on the Growth of 0-Year Olds." *Marine Biology* 92: 223–29.
- Ochi, H. 1989. "Mating Behavior and Sex Change of the Anemonefish, *Amphiprion clarkii*, in the Temperate Waters of Southern Japan." *Environmental Biology of Fishes* 26: 257–275.
- Paris, C. B., L. M. Chérubin, and R. K. Cowen. 2007. "Surfing, Spinning, or Diving from Reef to Reef: Effects on Population Connectivity." *Marine Ecology Progress Series* 347: 285–300.
- Paris, C. B., and R. K. Cowen. 2004. "Direct Evidence of a Biophysical Retention Mechanism for Coral Reef Fish Larvae." *Limnology and Oceanography* 49: 1964–79.
- Pinsky, M., E. J. Drenkard, and E. Curchitser. 2023. "CamotesROMS Surface Currents." Figshare. Dataset. <https://doi.org/10.6084/m9.figshare.22827059.v1>
- Pringle, J. M., A. M. H. Blakeslee, J. E. Byers, and J. Roman. 2011. "Asymmetric Dispersal Allows an Upstream Region to Control Population Structure throughout a species' Range." *Proceedings of the National Academy of Sciences of the United States of America* 108(15288–15): 293.
- Pusack, T. J., M. R. Christie, D. W. Johnson, C. D. Stallings, and M. A. Hixon. 2014. "Spatial and Temporal Patterns of Larval Dispersal in a Coral-Reef Fish Metapopulation: Evidence of Variable Reproductive Success." *Molecular Ecology* 23: 3396–3408.
- R Core Team. 2019. *R: A Language and Environment for Statistical Computing*. Vienna: R Foundation for Statistical Computing. <https://www.R-project.org/>.
- Resasco, J., and R. J. Fletcher. 2021. "Accounting for Connectivity Alters the Apparent Roles of Spatial and Environmental Processes on Metacommunity Assembly." *Landscape Ecology* 36: 1089–99.
- Rienecker, M. M., M. J. Suarez, R. Gelaro, R. Todling, J. Bacmeister, E. Liu, M. G. Bosilovich, et al. 2011. "MERRA: NASA's Modern-Era Retrospective Analysis for Research and Applications." *Journal of Climate* 24: 3624–48.
- Riginos, C., and L. Liggins. 2013. "Seascape Genetics: Populations, Individuals, and Genes Marooned and Adrift." *Geography Compass* 7: 197–216.
- Saenz-Agudelo, P., G. P. Jones, S. R. Thorrold, and S. Planes. 2012. "Patterns and Persistence of Larval Retention and Connectivity in a Marine Fish Metapopulation." *Molecular Ecology* 21: 4695–4705.
- Schunter, C., J. Carreras-Carbonell, E. Macpherson, J. Tintoré, E. Vidal-Vijande, A. Pascual, P. Guidetti, and M. Pascual. 2011. "Matching Genetics with Oceanography: Directional Gene Flow in a Mediterranean Fish Species." *Molecular Ecology* 20: 5167–81.
- Shoemaker, L. G., L. L. Sullivan, I. Donohue, J. S. Cabral, R. J. Williams, M. M. Mayfield, J. M. Chase, et al. 2020. "Integrating the Underlying Structure of Stochasticity into Community Ecology." *Ecology* 101: e02922.
- Siegel, D. A., S. Mitarai, S. D. Gaines, C. J. Costello, B. E. Kendall, R. R. Warner, and K. B. Winters. 2008. "The Stochastic Nature of Larval Connectivity among Nearshore Marine Populations." *Proceedings of the National Academy of Sciences of the United States of America* 105: 8974–79.
- Simons, R. D., D. A. Siegel, and K. S. Brown. 2013. "Model Sensitivity and Robustness in the Estimation of Larval Transport: A Study of Particle Tracking Parameters." *Journal of Marine Systems* 119–120: 19–29.
- Simpson, S. D., M. G. Meekan, N. J. Larsen, R. D. McCauley, and A. Jeffs. 2010. "Behavioral Plasticity in Larval Reef Fish: Orientation Is Influenced by Recent Acoustic Experiences." *Behavioral Ecology* 21: 1098–1105.

- Stillman, A. N., T. J. Lorenz, R. B. Siegel, R. L. Wilkerson, M. Johnson, and M. W. Tingley. 2022. "Conditional Natal Dispersal Provides a Mechanism for Populations Tracking Resource Pulses after Fire." *Behavioral Ecology* 33: 27–36.
- Sullivan, L. L., M. J. Michalska-Smith, K. P. Sperry, D. A. Moeller, and A. K. Shaw. 2021. "Consequences of Ignoring Dispersal Variation in Network Models for Landscape Connectivity." *Conservation Biology* 35: 944–954.
- Tigano, A., and V. L. Friesen. 2016. "Genomics of Local Adaptation with Gene Flow." *Molecular Ecology* 25: 2144–64.
- Watson, J. R., S. Mitarai, D. A. Siegel, J. E. Caselle, C. Dong, and J. C. McWilliams. 2010. "Realized and Potential Larval Connectivity in the Southern California Bight." *Marine Ecology Progress Series* 401: 31–48.
- White, C., K. A. Selkoe, J. R. Watson, D. A. Siegel, D. C. Zacherl, and R. J. Toonen. 2010. "Ocean Currents Help Explain Population Genetic Structure." *Proceedings of the Royal Society B: Biological Sciences* 277: 1685–94.
- White, J. W., M. H. Carr, J. E. Caselle, L. Washburn, C. B. Woodson, S. R. Palumbi, P. M. Carlson, et al. 2019. "Connectivity, Dispersal, and Recruitment: Connecting Benthic Communities and the Coastal Ocean." *Oceanography* 32: 50–59.
- Wolanski, E., D. Burrage, and B. King. 1989. "Trapping and Dispersion of Coral Eggs around Bowden Reef, Great Barrier Reef, Following Mass Coral Spawning." *Continental Shelf Research* 9: 479–496.
- Xie, S.-P., K. Hu, J. Hafner, H. Tokinaga, Y. Du, G. Huang, and T. Sampe. 2009. "Indian Ocean Capacitor Effect on Indo-Western Pacific Climate during the Summer Following El Niño." *Journal of Climate* 22: 730–747.

## SUPPORTING INFORMATION

Additional supporting information can be found online in the Supporting Information section at the end of this article.

**How to cite this article:** Catalano, Katrina A., Elizabeth J. Drenkard, Enrique N. Curchitser, Allison G. Dedrick, Michelle R. Stuart, Humberto R. Montes Jr., and Malin L. Pinsky. 2024. "The Contribution of Nearshore Oceanography to Temporal Variation in Larval Dispersal." *Ecology* 105(10): e4412. <https://doi.org/10.1002/ecy.4412>